

## Effects of Ti underlayer on the degree of order of Fe<sub>50</sub>Pt<sub>50</sub> films

S.C. Chen<sup>a,b,\*</sup>, P.C. Kuo<sup>a</sup>, S.T. Kuo<sup>a</sup>, A.C. Sun<sup>a</sup>, C.T. Lie<sup>a</sup>, C.Y. Chou<sup>a</sup>

<sup>a</sup> Institute of Materials Science and Engineering, National Taiwan University, Taipei, Taiwan

<sup>b</sup> Department of Mechanical Engineering, De Lin Institute of Technology, Taipei, Taiwan

Received 23 September 2002; received in revised form 6 January 2003; accepted 27 January 2003

### Abstract

Fe<sub>50</sub>Pt<sub>50</sub>/Ti double-layer films were deposited on corning 1737F glass substrates by d.c. magnetron sputtering of FePt and Ti targets. The magnetic layer FePt was deposited at substrate temperature of 600 °C in order to get ordered  $\gamma_1$ -FePt hard magnetic phase. It is found that the degree of order ( $S$ ) of FePt layer increases with increasing Ti underlayer thickness. The  $S$  value for FePt single-layer film is about 0.68, and it increases to about 0.76 as the thickness of the Ti underlayer increases to 150 nm. The average grain size of the FePt film is largely reduced as the Ti underlayer is introduced. The average grain size of the single-layer FePt film is about 25 nm, it will reduced to about 12 nm as 30 nm Ti underlayer is introduced, but the average grain size of FePt is increased as the thickness of Ti underlayer is increased. Magnetic measurement indicates that the in-plane coercivity ( $H_{c\parallel}$ ) of the FePt film increases with increasing thickness of Ti underlayer, but the in-plane squareness ( $S_{\parallel}$ ) decreases.

© 2003 Elsevier Science B.V. All rights reserved.

**Keywords:** Magnetron sputtering; Fe<sub>50</sub>Pt<sub>50</sub>/Ti double-layer films; Magnetic properties; Degree of order

### 1. Introduction

The FePt thin films with L1<sub>0</sub> ordered structure have received extensive attention due to their extremely high magnetic anisotropy constant  $K_u$ . The  $K_u$  value of fully ordered FePt alloy can be as high as  $7 \times 10^7$  erg cm<sup>-3</sup> [1,2]. Generally, the crystal structure of FePt film which deposits at room temperature is face-centered cubic (f.c.c.)  $\gamma$ -FePt disordered phase and shows soft magnetic behavior [3,4]. This disordered f.c.c.  $\gamma$ -FePt phase can be transformed to hard magnetic face-centered-tetragonal (f.c.t.)  $\gamma_1$ -FePt ordered phase after annealing at high temperature [4,5]. Therefore,  $H_c$  value of the FePt film is dependent on the degree of order of the film, i.e., the content of ordered  $\gamma_1$ -FePt phase in the film. When the f.c.c.  $\gamma$ -FePt phase transforms to the  $\gamma_1$ -FePt phase, the lattice parameter is contractive along the  $c$ -axis, resulting in a  $c/a$  ratio less than unity. The  $c/a$  ratio is 0.956 for fully ordered  $\gamma_1$ -FePt phase [6]. The degree of order of the FePt film is increased as  $c/a$  ratio is decreased.

It has been shown that the introduction of Ti underlayer would improve the out-plane magnetic properties of the CoCrPt magnetic recording films [7,8]. In this work, we investigated the effects of Ti underlayer on the degree of order, microstructure and magnetic properties of the magnetic FePt layer, which was deposited on heated substrate in order to form ordered  $\gamma_1$ -FePt hard magnetic phase directly [9].

### 2. Experimental

The Fe<sub>50</sub>Pt<sub>50</sub>/Ti double-layer film was sputtered on corning 1737F glass substrate by using high-purity FePt (99.99%) and Ti (99.99%) targets with d.c. magnetron sputtering. The magnetic layer FePt was deposited at substrate temperature of 600 °C in order to get ordered  $\gamma_1$ -FePt hard magnetic phase. The thickness of Ti underlayer was varied from 30 to 150 nm and the magnetic layer was fixed at 300 nm. Thickness of Ti underlayer was controlled by varying sputtering time. The substrate was rotated at 38 rpm in order to attain a uniform composition of FePt/Ti double films. A layer of SiN<sub>x</sub> with 30 nm thickness was covered on the magnetic film to avoid the oxidation of magnetic layer.

\* Corresponding author. Tel.: +886-2-2364-8881; fax: +886-2-2363-4562.

E-mail address: sscchh@ms28.hinet.net (S.C. Chen).

The base pressure of sputtering chamber was around  $3 \times 10^{-7}$  Torr. The sputtering power for Ti underlayer was 120 W and the sputtering Ar pressure was fixed at 3 mTorr after introducing high-purity argon (99.999%). The sputtering power for FePt magnetic layer was 40 W and Ar pressure was 10 mTorr.

Magnetic properties of the film were measured by using vibrating sample magnetometer (VSM) with maximum applied field of 12 kOe. Structure of the film was determined by X-ray diffractometer (XRD). The film microstructure was observed by field emission scanning electron microscopy (FE-SEM). Grain size of the film was derived from the XRD diffraction peak based on Scherrer equation. The composition and homogeneity of the magnetic film were analyzed by energy-dispersive spectrum (EDS). The film thickness was measured by atomic force microscope (AFM) and  $\alpha$ -step.

### 3. Results and discussion

Fig. 1 shows the XRD patterns of  $\text{Fe}_{50}\text{Pt}_{50}/\text{Ti}$  films with different Ti underlayer thickness. As thickness of the Ti underlayer increases from 0 to 50 nm, intensity of the peak Ti(0 0 2) become stronger and the peak of Ti(1 0 0) appear. However, the (0 0 1) and (1 1 0) diffraction peaks of  $\gamma_1$ -FePt phase disappear and intensity of the  $\gamma_1$ -FePt (1 1 1) peak is raised. Intensity of the  $\gamma_1$ -FePt (1 1 1) peak increases as the Ti underlayer thickness is further increased from 50 to 150 nm. This

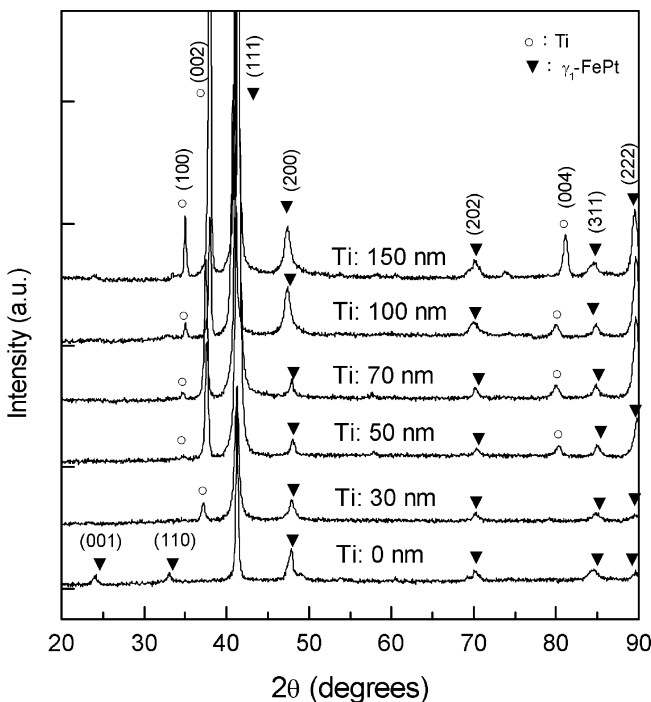


Fig. 1. The XRD patterns of various  $\text{Fe}_{50}\text{Pt}_{50}/\text{Ti}$  films with different Ti underlayer thickness. The thickness of FePt layer is fixed at 300 nm.

indicates that the amount of  $\gamma_1$ -FePt phase in the FePt layer increases and the preferred orientation of  $\gamma_1$ -FePt (1 1 1) is induced as the thickness of Ti underlayer is increased.

Fig. 2 shows the average grain sizes of FePt layer and Ti layer as a function of Ti underlayer thickness. The grain sizes of FePt and Ti are calculated from Scherrer equation [10] by using the diffraction peaks of  $\gamma_1$ -FePt (1 1 1) and Ti (0 0 2), respectively. We can see that the grain sizes of FePt and Ti are increased with increasing Ti underlayer thickness. Average grain size of the Ti underlayer increases from 18.2 to 27.1 nm and the average grain size of the FePt layer increases from 11.6 to 24 nm as thickness of Ti underlayer increases from 30 to 150 nm. Average grain size of FePt without Ti underlayer is 24.3 nm. However, the grain size of FePt decreases sharply from 24.3 to 11.6 nm as 30 nm of Ti underlayer is introduced. The decrease of FePt grain size when Ti underlayer is introduced is because the grain growth of FePt is along the grain of Ti underlayer. The grain size of FePt is controlled by the grain size of Ti underlayer. Since, the grain size of Ti increases with increasing Ti layer thickness as shown in Fig. 2, the grain size of FePt also increases with increasing Ti layer thickness.

Fig. 3 shows the FE-SEM micrograph of the cross-section of the  $\text{SiN}_x/\text{FePt}/\text{Ti}$  film with Ti underlayer thickness of 100 nm. Since the sample is tilted slightly during preparation, the thickness of  $\text{SiN}_x$  layer looks like larger than 30 nm. The Ti underlayer grows to columnar grain which is perpendicular to the film plane and the XRD analysis of Fig. 1 shows that the preferred orientation of Ti underlayer is [0 0 2]. The grain growth of FePt is along the grain of Ti underlayer initially, columnar grains of FePt disappear and become ran-

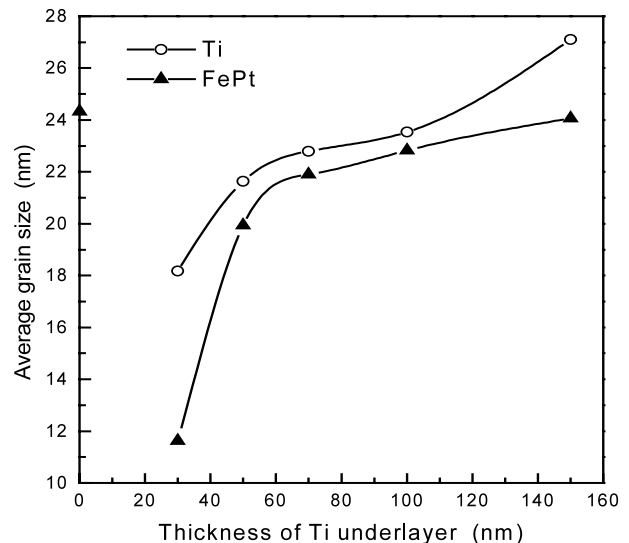


Fig. 2. The average grain sizes of FePt layer and Ti layer as a function of Ti underlayer thickness.

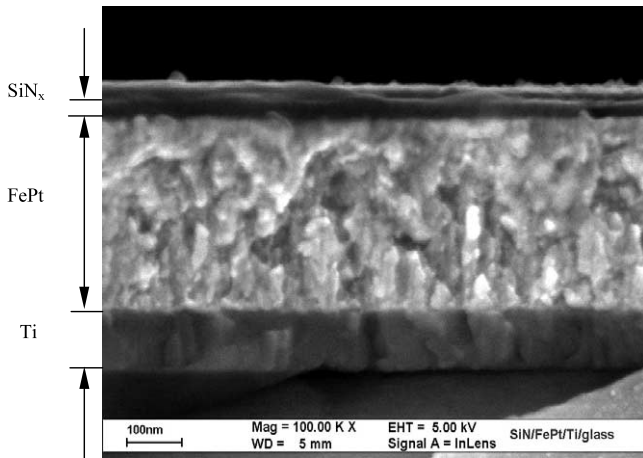


Fig. 3. FE-SEM micrograph of the cross-section of the  $\text{SiN}_x/\text{FePt}/\text{Ti}$  film. Thickness of  $\text{SiN}_x$ , FePt and Ti layers are 30, 300 and 100 nm, respectively.

domly orientated when FePt layer is thicker than about 150 nm as shown in Fig. 3.

The degree of order ( $S$ ) of the FePt magnetic layer will affect the magnetic properties of FePt/Ti double-layer films. The  $c/a$  values of partially ordered FePt films with different thickness of Ti underlayer were determined by using the X-ray diffraction peaks of (1 1 1) and (2 0 0) of  $\gamma_1$ -FePt phase. Degree of order of the FePt layer can be obtained and expressed as [11]:

$$S^2 = \frac{1 - c/a}{1 - (c/a)_{S_f}}$$

where  $(c/a)_{S_f}$  is the  $c/a$  value of fully ordered FePt film, it is 0.956 [6].  $(c/a)$  is the value of partially ordered FePt film. Fig. 4 shows the degree of order as a function of Ti underlayer thickness. The result shows the degree of order of FePt film increases with increasing the thick-

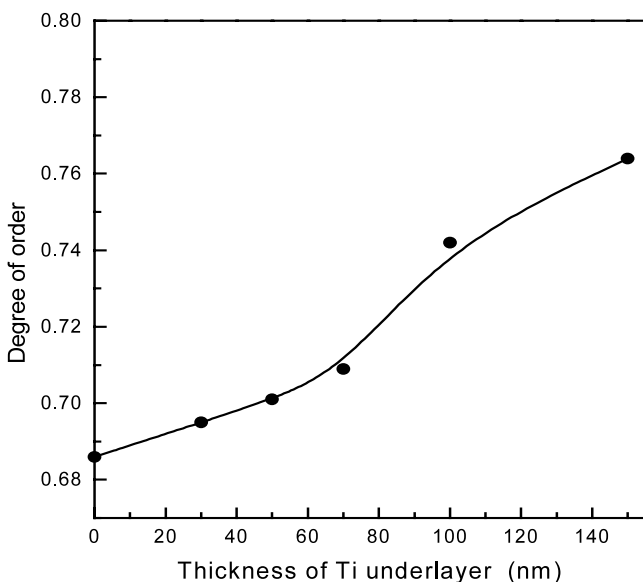


Fig. 4. The degree of order of FePt film as a function of the thickness of Ti underlayer in FePt/Ti film.

ness of Ti underlayer. This means that the introduction of Ti underlayer and an increase in Ti underlayer thickness will increase the degree of order of the FePt film. The degree of order of FePt film without Ti underlayer is 0.684. However, it increases to 0.741 as the thickness of Ti underlayer is 100 nm, as shown in Fig. 4. When the thickness of Ti underlayer is further increased from 100 to 150 nm, the degree of order of FePt film increases from 0.741 to 0.762. The increase in the degree of order of FePt film is due to the grain sizes of Ti underlayer and FePt layer increase with increasing the thickness of Ti underlayer, as shown in Fig. 2. Wong et al. [12] had shown that the degree of interfacial misfit is larger as the grain size is larger in Co/Cr film, and this will introduce stacking fault and misfit dislocation into the Co layer in order to reduce the degree of interfacial misfit, and the phase transformation is easier owing to the existence of these defects. Similarly, in our FePt/Ti system, the introduction of these defects in the FePt layer will make the transformation of  $\gamma$ -FePt into  $\gamma_1$ -FePt phase easier. Therefore, the degree of order of FePt layer is increased with increasing Ti underlayer thickness, i.e., the grain size of Ti, as shown in Fig. 4.

Fig. 5 shows the in-plane coercivity ( $H_{c\parallel}$ ) and perpendicular coercivity ( $H_{c\perp}$ ) as function of the Ti underlayer thickness. It indicates that  $H_{c\parallel}$  and  $H_{c\perp}$  of the film increase with increasing thickness of Ti underlayer. For the FePt single-layer film without Ti underlayer,  $H_{c\parallel}$  and  $H_{c\perp}$  are 3.1 and 2.3 kOe, respectively. As the thickness of Ti underlayer increases to 100 nm,  $H_{c\parallel}$  and  $H_{c\perp}$  will increase to 7.3 and 4.2 kOe, respectively. Since increasing the thickness of Ti underlayer will enhance the degree of order of FePt layer, i.e., increase the amount of  $\gamma_1$ -FePt phase in the FePt layer, the in-

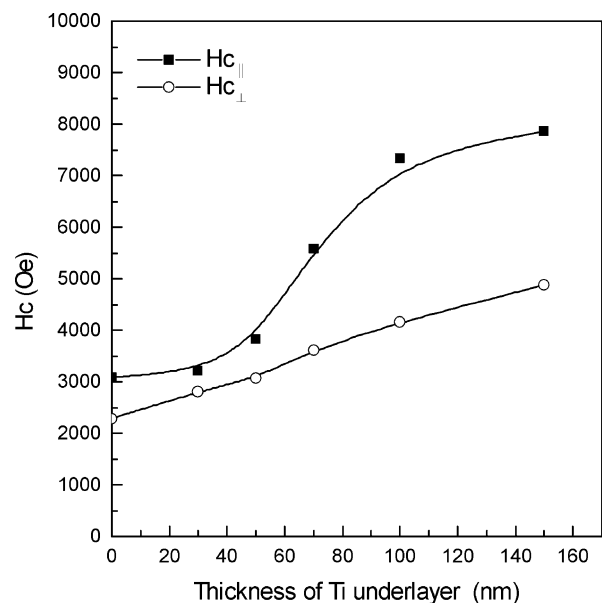


Fig. 5.  $H_{c\parallel}$  and  $H_{c\perp}$  of the FePt/Ti film as a function of Ti underlayer thickness.

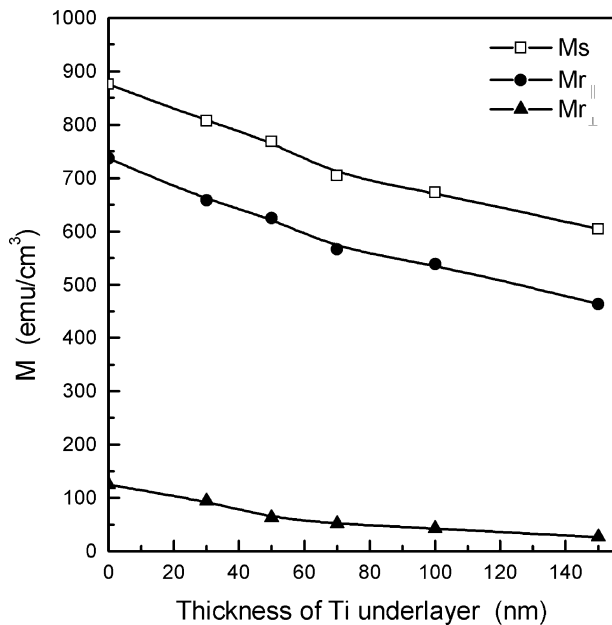


Fig. 6.  $M_s$ ,  $M_{r\parallel}$  and  $M_{r\perp}$  of the FePt/Ti film as a function of the thickness of Ti underlayer.

plane and perpendicular coercivity of the film are increased.

Fig. 6 shows the saturation magnetization ( $M_s$ ), in-plane remnant magnetization ( $M_{r\parallel}$ ) and perpendicular remnant magnetization ( $M_{r\perp}$ ) of the FePt/Ti films as a function of the Ti underlayer thickness. It shows that  $M_s$ ,  $M_{r\parallel}$  and  $M_{r\perp}$  of the film decrease with increasing thickness of Ti underlayer. For FePt single-layer film without Ti underlayer, the  $M_s$ ,  $M_{r\parallel}$  and  $M_{r\perp}$  values are 875, 736 and 124  $\text{emu cm}^{-3}$ , respectively.  $M_s$ ,  $M_{r\parallel}$  and  $M_{r\perp}$  values will decrease to 672, 538 and 50  $\text{emu cm}^{-3}$ , respectively, as 100 nm Ti underlayer is introduced. The

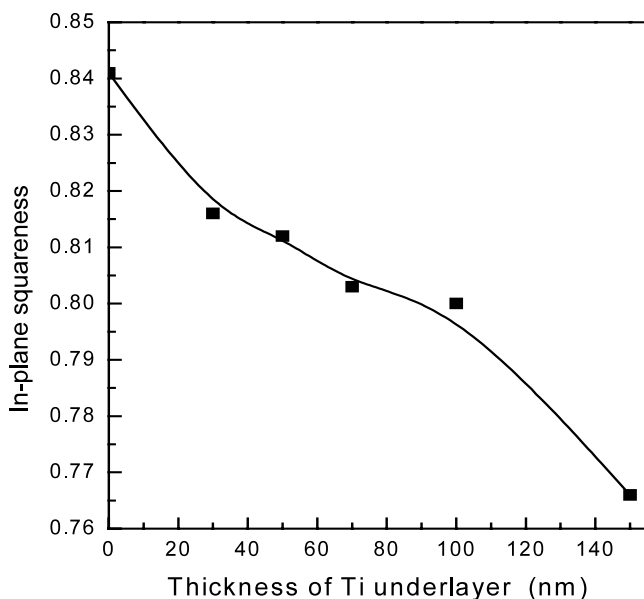


Fig. 7. The relationship between in-plane squareness and the thickness of Ti underlayer of FePt/Ti film.

decrease in magnetization of FePt layer with increasing Ti underlayer thickness is mainly due to the increase of  $\gamma_1$ -FePt phase content in the film, because the  $M_s$  value of  $\gamma_1$ -FePt phase is lower than that of  $\gamma$ -FePt phase [13].

Fig. 7 shows the relationship between in-plane squareness ( $S_{\parallel}$ ) and the thickness of Ti underlayer of the FePt/Ti film.  $S_{\parallel}$  is defined as the ratio of  $M_{r\parallel}$  to  $M_s$ . It shows that  $S_{\parallel}$  decreases with increasing Ti underlayer thickness.  $S_{\parallel}$  value is 0.84 for the FePt single-layer film without Ti underlayer. As the thickness of Ti underlayer increases from 0 to 100 nm,  $S_{\parallel}$  decreases from 0.84 to 0.8. Obviously, thicker Ti underlayer has not favored the in-plane squareness of FePt/Ti film.

#### 4. Conclusions

The conclusions are as follows: (1) The degree of order and  $H_{c\parallel}$  of the FePt/Ti double-layer films, both increase with increasing thickness of Ti underlayer, and (2) although the increase of Ti underlayer thickness enhances the degree of order of the FePt layer in FePt/Ti film, the in-plane squareness and saturation magnetization decrease with increasing thickness of Ti underlayer.

#### Acknowledgements

This work was supported by the National Science Council of ROC through Grant No. NSC90-2216-E-002-036.

#### References

- [1] K. Watanabe, H. Masumoto, *Trans. Jpn. Inst. Met.* 24 (1983) 627.
- [2] M. Watanabe, T. Nakayama, K. Watanabe, T. Hirayama, A. Tonomura, *Mater. Trans. JIM* 37 (1996) 489.
- [3] J.A. Aboaf, T.R. McGuire, S.R. Herd, E. Klokholm, *IEEE Trans. Magn.* 20 (1984) 1642.
- [4] S.C. Chen, P.C. Kuo, A.C. Sun, C.T. Lie, W.C. Hsu, *Mater. Sci. Eng. B* 88 (2002) 91.
- [5] K. Watanabe, *Mater. Trans. JIM* 32 (1991) 292.
- [6] P. Villas, L.D. Calvert, *Pearson's Handbook of Crystallographic Data for Intermetallic Phase*, vol. 4, ASM Information, 1991.
- [7] I.S. Lee, H. Ryu, H.J. Lee, T.D. Lee, *J. Appl. Phys.* 85 (1999) 6133.
- [8] B. Lu, T. Klemmer, S. Khizroev, J.K. Howard, D. Litvinov, A.G. Roy, D.E. Laughlin, *IEEE Trans. Magn.* 37 (2001) 1319.
- [9] S. Jeong, T. Ohkubo, A.G. Roy, D.E. Laughlin, M.E. McHenry, *J. Appl. Phys.* 91 (2002) 6863.
- [10] B.D. Cullity, *Elements of X-ray Diffraction*, 2nd ed., Addison-Wesley, Reading, MA, 1978.
- [11] B.W. Roberts, *Acta Metall.* 2 (1954) 597.
- [12] B.Y. Wong, J.F. Ying, K. Johnson, *IEEE Trans. Magn.* 36 (2000) 2360.
- [13] T. Katayama, T. Sugimoto, Y. Suzuki, M. Hashimoto, P. de Haan, J.C. Lodder, *J. Magn. Mater.* 104–107 (1992) 1002.